Thermal Evolution of the Cl^-−$LiAl_2$ Layered Double Hydroxide: A Multinuclear MAS NMR and XRD Perspective

Xiaoqiang Hou* and R. James Kirkpatrick

Department of Geology, University of Illinois at Urbana-Champaign, Urbana, Illinois 61801

Received June 25, 2001

Layered double hydroxides (LDHs) with a cation composition of $LiAl_2$ have a wide range of potential applications as catalysts, catalyst supports, and precursors for refractory oxide materials, including several industrially important lithium aluminate phases. The understanding of the calcination behavior of this group of LDH phases is essential to advancing these applications, and the research described here focuses on the thermal decomposition and structural evolution of $LiAl_2(OH)_6Cl{\cdot}nH_2O$ in the temperature range of 20−1100 °C. ^{27}Al, ^{35}Cl, and $^{6,7}Li$ magic angle spinning nuclear magnetic resonance spectroscopy, powder X-ray diffraction, thermal analysis (including thermogravimetric and differential scanning calorimetry), and compositional analysis provide a highly consistent picture of the thermally induced phase formation and transformations of this LDH. The loss of the surface and interlayer water can begin as low as room temperature, depending on the relative humidity. Beginning at about 300 °C, the simultaneous volatilization of H_2O and HCl and the exsolution of crystalline LiCl result in the formation of amorphous Li−Al−O−OH. By at least 500 °C, volumes with the structures of α-$LiAlO_2$ and $LiAl_5O_8$ appear, and these phases become progressively more ordered with increasing temperature. LiCl begins to volatilize by 850 °C and is present only in trace amounts above ca. 1000 °C. α-$LiAlO_2$ converts to γ-$LiAlO_2$ between 970 and 1100 °C. Because of the delithiation due to LiCl volatilization, the final products are dominated by $LiAl_5O_8$, in contrast to the calcination products of previously studied $LiAl_2$ LDHs which are dominated by $LiAlO_2$.

Introduction

The understanding of the structural and compositional evolution of layered double hydroxides (LDHs) with progressive calcination at elevated temperatures is essential to advancing their use as catalysts, catalysts precursors, and precursors for refractory oxide materials.[1−3] We present here comprehensive X-ray diffraction (XRD), thermogravimetric/differential scanning calorimetry (TG/DSC), and multinuclear NMR data that explore the thermal evolution of the chloride containing the $LiAl_2$ LDH compound $LiAl_2(OH)_6Cl{\cdot}nH_2O$. The end products of its thermal decomposition, α- and γ-$LiAlO_2$ and $LiAl_5O_8$, are important ceramic phases which have potential applications in nuclear fusion reactors[4] as electrolyte matrixes,[4] in plant illumination[5,6] as catalyst supports, and in the preparation of delithiated alumina compounds.[1−3] The thermal evolution of similar $LiAl_2$ LDH phases, $LiAl_2(OH)_6NO_3{\cdot}nH_2O$,[7] $LiAl_2(OH)_6(CO_3)_{0.5}{\cdot}nH_2O$,[8] and $LiAl_2(OH)_6OH{\cdot}nH_2O$,[1,7] has been previously examined using primarily XRD. Here, the combination of ^{27}Al, ^6Li, ^7Li, and ^{35}Cl NMR spectroscopies at a very high field (H_0 = 17.6 T), XRD, TG/DSC, and compositional analysis provides a far more complete picture of the phase formation, phase transformations, and compositional changes occurring at elevated temperatures. Most importantly, the ^{27}Al, ^6Li, ^7Li, and ^{35}Cl NMR data provide detailed local structural information for both the well-crystallized phases and the amorphous and poorly crystallized intermediate phases. The results define the temperature ranges over which evolutionary events including dehydration, dehydroxylation, dechlorination, delithiation, and the crystallization and structural reorganization of α- and γ-$LiAlO_2$ and $LiAl_5O_8$ occur. Because of the delithiation and dechlorination specific to the $LiAl_2(OH)_6Cl{\cdot}nH_2O$ compound, the amount of $LiAl_5O_8$ in the final calcination products is about 3.1 times that of γ-$LiAlO_2$, which is the dominant product in the calcined nitrate, carbonate, and hydroxyl forms.[1,7,8]

LDHs are layer-structured hydroxides that have a permanent, positive layer charge and, thus, a significant anion-exchange capacity due to isomorphous substitution, most commonly in the hydroxide layers.[9] The crystal structures of most LDHs consist of positively charged hydroxide sheets separated by interlayers containing exchangeable anions and water molecules.[9−11] The $LiAl_2$ LDH compounds develop a positive charge because of the substitution of Li^+ for the vacancies of a dioctahedral gibbsite sheet, and the Li and Al are well ordered.[11] At room temperature, the interlayer Cl^- is well ordered in the anhydrous phase, but in the hydrated phase, the Cl^- and water molecules are positionally disordered.[12]

* To whom correspondence should be addressed. Phone: (217) 244-2355. Fax: (217) 244-4996. E-mail: xhou@uiuc.edu.

(1) Nayak, M.; Kutty, T. R. N.; Jayaraman, V.; Periaswamy, G. *J. Mater. Chem.* **1997**, *7* (10), 2131−2137.
(2) Jimenez-Becerril, J.; Bosch, P.; Bulbilian, S. *J. Nucl. Mater.* **1991**, *185*, 304−307.
(3) Poeppelmeier, K. R.; Chiang, C. K.; Kipp, D. O. *Inorg. Chem.* **1988**, *27*, 4523−4526.
(4) Alessandrini, F.; Alvani, C.; Casasio, S.; Mancini, M. R.; Nannetti, C. A. *J. Nucl. Mater.* **1995**, *224*, 236−244.
(5) Kutty, T. R. N.; Nayak, M. *Mater. Res. Bull.* **1999**, *34* (2), 249−262.
(6) Kutty, T. R. N.; Nayak, M. *J. Alloys Compd.* **1998**, *269*, 75−87.
(7) Poeppelmeier, K. R.; Hwu, S.-J. *Inorg. Chem.* **1987**, *26*, 3297−3302.
(8) Hernandez, M. J.; Ulibarri, M. A. *Thermochim. Acta* **1985**, *94*, 257−266.
(9) Cavani, F.; Trifiro, F.; Vaccari, A. *Catal. Today* **1991**, *11*, 173.
(10) Serna, C. J.; White, J. *Clays Clay Miner.* **1977**, *25*, 384−391.
(11) Serna, C. J.; Rendon, J. L.; Iglesias, J. E. *Clays Clay Miner.* **1982**, *30* (3), 180−184.
(12) Besserguenev, A. V.; Fogg, A. M.; Francis, R. J.; Price, S. J.; O'Hare, D. *Chem. Mater.* **1997**, *9*, 241−247.

10.1021/ic010671d CCC: $20.00
Published on Web 10/30/2001

Experimental Section

Sample Preparation. $LiAl_2(OH)_6Cl{\cdot}nH_2O$ samples were prepared by the direct reaction of gibbsite with a LiCl solution.[13] For each sample, 9 g of gibbsite and 15 g of LiCl were mixed with 25 mL of boiled deionized (DI) water, and the mixture was reacted at 90 °C for 14 h in a tightly sealed polyethylene bottle under strong stirring. The suspension was centrifugally separated and ultrasonically washed for three cycles using boiled DI water to remove the excess LiCl. The sample used here (LiAlCl8) was then dried in a vacuum at room temperature for several weeks. A high concentration of LiCl (14 M in our case) is critical in the preparation of $LiAl_2(OH)_6Cl{\cdot}nH_2O$ by this method. Fogg and O'Hare[13] reported that the rate of the reaction is half-order with respect to the initial concentration of LiCl. Our experience shows that a significant formation of $LiAl_2(OH)_6Cl{\cdot}nH_2O$ using 0.5 M LiCl under conditions similar to those described previously does not occur.

Calcination was conducted using the following methods. For temperatures of 720 °C and below, aliquots of dried LiAlCl8 were placed in a furnace at the desired temperature and heated for 6 h in air. For temperatures of 850 °C and above, samples were placed in the furnace at 850 °C, the furnace was ramped to the desired calcination temperature over a few minutes, and the sample was held at the run temperature for 3 h. In all of the cases, the samples were heated in open Pt crucibles in air, allowed to cool to 200 °C in the furnace, and then quickly removed to a desiccator with P_2O_5. After being cooled to room temperature, five aliquots of the sample were stored in separate vials in a glovebag for parallel XRD, NMR, and elemental analysis.

Sample Examination. Samples were examined by elemental analysis, XRD, TG, DSC, and ^{27}Al , ^{6}Li, ^{7}Li, and ^{35}Cl MAS NMR. For elemental analysis, Li and Al and were determined using inductively coupled plasma-atomic emission spectroscopy (ICP-AES), C and H were determined with a CHN analyzer, and Cl^- was determined by titration. Dissolution of the refractory high-temperature calcination products was difficult, and these samples were dissolved in a mixture of phosphoric and sulfuric acids at ~250 °C for analysis. TG and DSC data were recorded from room temperature to 1225 °C at a heating rate of 10 °C min^{-1} in both Ar and air using a NETZSCH Simultaneous Thermal Analyzer STA 409. Powder XRD patterns were recorded with a Rigaku diffractometer using Cu Kα radiation at a scanning rate of 1° 2θ min^{-1} and a step size of 0.02° 2θ. No special precautions were taken to prevent a preferred orientation during sample loading or to prevent the absorption of moisture. The samples were exposed to ambient atmosphere during XRD data collection. The only apparent effect of this was in the hydration of crystalline LiCl. KGa-1 kaolinite (Clay Minerals Repository, University of Missouri, Columbia) was used as an external XRD standard.

^{27}Al and ^{35}Cl MAS NMR spectra were collected at room temperature using both a Varian 750 spectrometer (H_0 = 17.62 T) and a home-built 500 MHz spectrometer (H_0 = 11.74 T) equipped with Doty Scientific fast MAS probes. The calcined samples were quickly loaded from their sealed containers into capped rotors just prior to data collection to avoid moisture absorption. Aqueous solutions of 1 M $AlCl_3$ and 1 M NaCl were used as external chemical-shift standards for ^{27}Al and ^{35}Cl, respectively, and their chemical shifts were set at 0 ppm. The measured 90° pulses for both of the solutions, ^{27}Al and ^{35}Cl, were 8 μs. Shorter pulses of 1 μs for ^{27}Al and 3 μs for ^{35}Cl were used for the MAS NMR spectra of the solid samples to get better quantification. Typically, a recycle time of 1 s was used for both ^{27}Al and ^{35}Cl.

^{6}Li and ^{7}Li MAS NMR spectra were recorded using the Varian 750 instrument only. A 1 M LiCl aqueous solution was used as an external chemical-shift reference and set at 0 ppm. ^{6}Li has a spin of $I = 1$, low relative abundance (7.4%), and a surprisingly long T_1 but the smallest electric quadrupole moment of any quadrupolar nuclide.[14] Thus, its spectral lines are very narrow, and it often provides higher resolution than ^{7}Li.[14,15] This is the case here. The estimated 90° pulse for solution ^{6}Li is 8.2 μs on the basis of the pulse length of ^{2}H in $^{2}H_2O$ which has a similar Larmor frequency, and the ^{6}Li pulse length for the solids was 2 μs. The ^{6}Li recycle time for the spectra reported here was 60 s. There is no significant difference in the relative intensities of the ^{6}Li spectral components and their peak shapes between spectra collected with recycle times of 20 and 60 s. MAS spinning frequencies were 9.5−11 kHz. Normally, 80−300 scans were acquired for each spectrum. An exponential line broadening of 15 Hz was used to process the data with the NUTs processing package. Line simulation and integration were also performed using the NUTs software. ^{7}Li has a spin of $I = {}^3/_2$, a large natural abundance (92.6%) and nuclear receptivity, and a relatively small electric quadrupole moment.[14,15] For our samples, only one scan is required for good S/N ratios in the ^{7}Li spectra.

Results and Interpretation

Chemical Analysis. The structural formula of the sample used for the calcination experiments (LiAlCl8) based on compositional analysis is $Li_{0.970}Al_{2.030}(OH)_6Cl_{0.977}{\cdot}0.644H_2O$. This composition conforms closely to the desired stoichiometric composition of $LiAl_2(OH)_6Cl{\cdot}H_2O$ except that the analyzed water content depends significantly on the drying and storage conditions. Although LiCl was greatly in excess in the initial mixture, the Al/Li molar ratio of the final product is close to 2, consistent with a strict Al/Li ordering in the octahedral sheet. This observation is in contrast to Mg/Al LDHs (hydrotalcites) for which the final Al/Mg ratio can vary from $^1/_5$ to $^1/_2$ depending on the initial solution Al/Mg ratio and the synthesis route.[9] Here, the analyzed Al/Li ratio is slightly larger than 2 because of a small amount of gibbsite, as observed by XRD (Figure 1). LiAlCl8 contains the least amount of gibbsite of all of the samples that we synthesized and has an Al/Li ratio closest to 2. The gibbsite present could be unreacted starting material or could have formed by the leaching of the LDH product during washing.[7] No carbonate was detected in LiAlCl8, although contamination of LDHs by atmospheric CO_2 is common and was observed for our other samples.

Compositional analysis shows a significant decrease in the Cl content and an increase in the Al/Li molar ratio in the calcined samples. For the 850 °C sample, the elemental composition (wt %) is 43.01% Al, 3.88% Li, 2.54% Cl, 0.13% C, and 0.24% H and, for the 1100 °C sample, it is 49.25% Al, 2.80% Li, 1.09% Cl, 0.05% C, and 0.04% H. On the basis of these analyses, the atomic Al/Li ratios of these two samples are 2.85 and 4.52, respectively. These values are in good agreement with the line fits of the ^{6}Li NMR data, as discussed in the following paragraphs.

TG and DSC. The TG and DSC curves obtained in Ar and air are essentially identical, and only those under Ar are presented here (Figure 2). For the sample LiAlCl8 (Figure 2a), there are four well-defined endotherms with maxima at about 125, 355, 535, and 1020 °C, and each of these events has an associated weight loss except for that at 535 °C. The three observed weight loss events are readily assigned to the loss of physically adsorbed and structural (interlayer) water at 125 °C, dehydroxylation and partial dechlorination at 355 °C (see the discussion of NMR data that follows), and volitalization of LiCl at 1020 °C. The $LiAl_2$ LDH compounds are well-known to lose surface and interlayer water at quite low temperatures, and our peak near 125 °C is in good agreement with the previous data.[16] ^{35}Cl NMR and relative humidity (RH) controlled IR data (data not shown) also show that samples equilibrated over P_2O_5 for several days or that samples equilibrated in RH = 0% air for 2 h lose most of their surface and interlayer water. The 355 °C feature is relatively narrow for the dehydroxylation of an LDH,

(13) Fogg, A. M.; O'Hare, D. *Chem. Mater.* **1999**, *11*, 1771−1775.
(14) Xu, Z.; Stebbins, J. F. *Solid State Nucl. Magn. Reson.* **1995**, *5*, 103−112.
(15) Alam, T. M.; Conzone, S.; Brow, R. K.; Boyle, T. J. *J. Non-Cryst. Solids* **1999**, 140−154.
(16) Mascolo, G. *Thermochim. Acta* **1986**, *102*, 67−73.

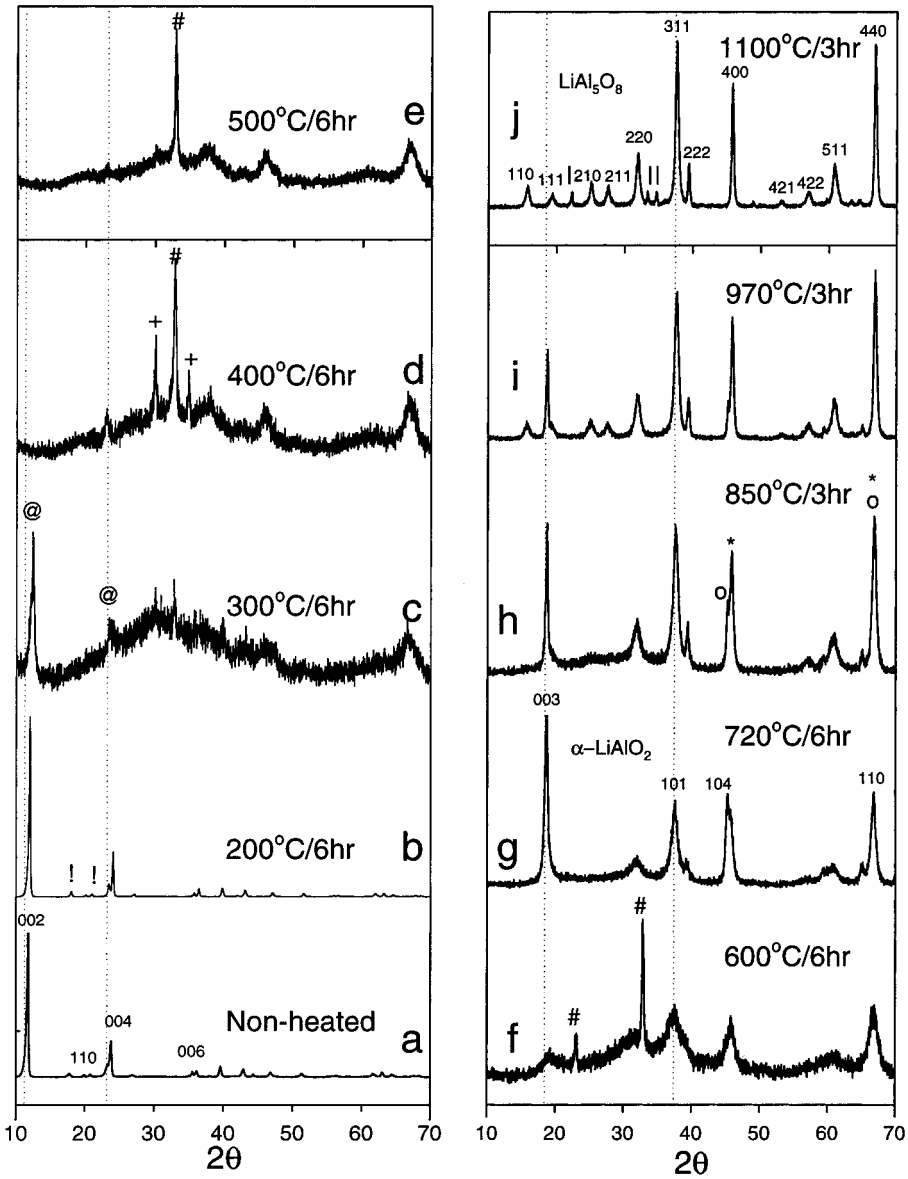

Figure 1. Powder XRD patterns of $LiAl_2(OH)_6Cl{\cdot}nH_2O$ (LiAlCl8) and its products calcinated under the conditions indicated. The data were collected under ambient atmospheric conditions after the samples were cooled. Miller indexes in a, g, and j are for LDH, α-$LiAlO_2$, and $LiAl_5O_8$, respectively. Figure a is for the vacuum-dried nonheated sample. Legend: (@) LDH, (!) gibbsite, (+) LiCl, (#) $LiCl{\cdot}H_2O$, (○) α-$LiAlO_2$, (|) γ-$LiAlO_2$, (*) $LiAl_5O_8$.

implying energetically uniform hydroxyl and chloride environments as expected from the well-ordered Al/Li arrangement. The comparable peak for gibbsite is at about 330 °C (Figure 2b), indicating that the incorporation of LiCl into gibbsite increases the dehydroxylation temperature by ∼25 °C and that the LDH is slightly more stable than gibbsite, even in the absence of a LiCl solution. The highest-temperature weight loss actually starts near 850 °C and ends at 1050 °C. Its assignment to the volatilization of LiCl exsolved from the LDH is well confirmed by the XRD and ^{35}Cl and $^{6,7}Li$ MAS NMR data as shown in the following paragraphs. LiCl has a melting point of 610 °C and a boiling point of 1383 °C.[17] It readily volatilizes in air at temperatures lower than its boiling point, as indicated by the complete loss of LiCl salt when heated at 900 °C in an oven for 3 h.

The endothermic event at 540 °C is not associated with a weight loss and is probably due to a phase transition, which we describe in the following paragraphs. A feature for gibbsite in the same temperature range is associated with a weight loss and has been assigned to the dehydration of boehmite AlOOH, an intermediate phase in the formation of γ-Al_2O_3.[18] For our LDH sample, this feature is probably not due to an impurity in gibbsite because it is too large for the amount of gibbsite present.

XRD. The powder XRD patterns of our room temperature LDH samples are essentially identical to those previously published[11,19] (Figure 1). The data for the calcined samples show a significant breakdown of the LDH to both an amorphous or poorly crystalline material and to crystalline LiCl at 300 °C and also the formation of crystalline Li-aluminate phases at higher temperatures. Table 1 summarizes the phases identified at each temperature.

(17) Lide, D. R. *CRC Handbook of Chemistry and Physics*, 79th ed.; CRC Press: Boca Raton, FL, 1998.

(18) Yudin, R. N.; Ershova, K. S.; Umnova, E. G. In *Izuch. Str. Fazovogo Sostava Miner. Ob'ektov Kompleksom Fiz. Metodov Anal. Resheniya Geol. Zadach*; Solntseva, L. S., Krivokoneva, G. K., Eds.; VNII Miner Syr'ya: Moscow, Russian Federation, 1978; pp 63−81.

(19) Sissoko, I.; Iygba, E. T.; Sahai, R.; Biloen, P. *J. Solid State Chem.* **1985**, *60*, 283−288.

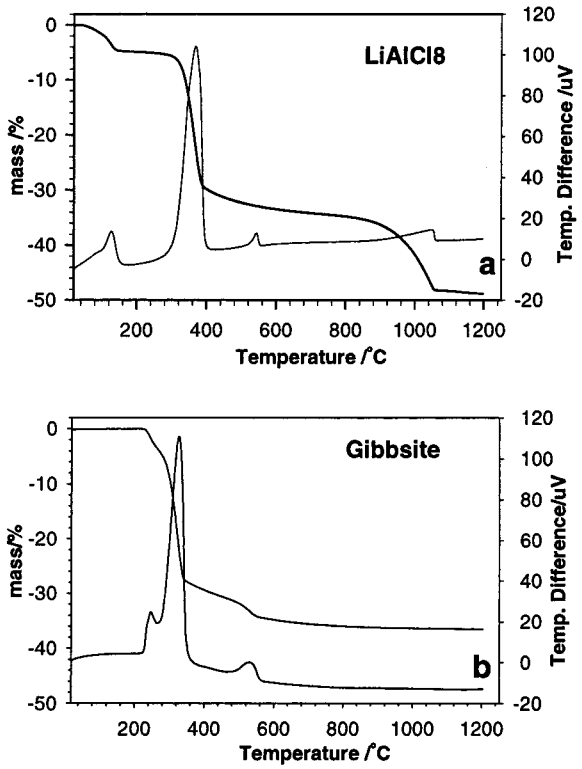

Figure 2. Thermal gravimetric (TG) analysis and differential scanning calorimetry (DSC) data for the $LiAl_2(OH)_6Cl{\cdot}nH_2O$ sample (LiAlCl8) and the gibbsite used to prepare it: (a) LiAlCl8; (b) gibbsite.

Table 1. Phases Identified in the Calcination of $LiAl_2(OH)_6Cl{\cdot}nH_2O$ and Their Observed ^{6}Li NMR Chemical Shifts[a], fwhh's, and Temperature Ranges

Li-containing phase	^{6}Li MAS chemical shift (ppm)	peak width, fwhh (Hz)	observed temperature range in this study
LiCl solution (1 M)	0 (reference)	62 (static)	N/A
LiCl solid	−1.10	36	300−970 °C
$LiCl{\cdot}H_2O$	−0.60	52	hydration product during XRD only
$LiAl_2(OH)_6Cl{\cdot}nH_2O$	−0.05	53−100	<100 °C
$LiAl_2(OH)_6Cl$	−0.07	71−95	100−300 °C
amorphous Li−Al−O−OH	−0.04 to −0.4	78−98	300−500 °C
α-$LiAlO_2$	−0.4	59−82	500−970 °C
γ-$LiAlO_2$	−0.06	55	∼1100 °C
$LiAl_5O_8$	0.31	46−93	500−1100 °C

[a] Peak maxima in MAS spectra at $H_0 = 17.6$ T.

(a) 300 °C and Below. For the vacuum-dried, unheated sample and the aliquot heated at 200 °C (parts a and b of Figure 1), the XRD patterns show the expected features of $LiAl_2(OH)_6Cl{\cdot}nH_2O$ with good crystallinity. Bragg peaks include sharp and intense (00*l*) basal reflections at low 2θ values and less intense (*hk*0) and (*hkl*) reflections at higher 2θ values. The indexing of the peaks here is based on a comparison to the reported refined patterns of a two-layer hexagonal superlattice.[11,19] The *d* spacing of the (002) reflection, which corresponds to the thickness of a single structural layer, is 7.80 Å for the initial wet paste, 7.56 Å for the sample dried over P_2O_5, and 7.42 Å for the sample heated at 200 °C for 6 h.

The powder XRD pattern of our 300 °C sample is significantly different than those for lower-temperature samples (Figure 1c). There is a broad hump from 20° to 50° 2θ and centered near 30° 2θ because of the development of a large fraction of an amorphous phase. Comparison to the DSC/TG data indicates that this phase change is due to partial dehydroxylation. The basal spacing of the residual LDH decreases to 7.20 Å, and its (00*l*) peaks broaden. Broad peaks are present near 46° and 66.6° 2θ. These two peaks are characteristic of Li/Al oxides, which we discuss later. The small peaks near 30° and 35° 2θ are due to LiCl (JCPCD 4-664) and those at 33° and 23° 2θ to its hydrate $LiCl{\cdot}H_2O$ (JCPCD 22-1142). Thus, the exsolution of LiCl from the LDH structure occurs simultaneously with dehydroxylation. The resulting LiCl is very hygroscopic[17] and easily adsorbs water from air to form the monohydrate phase.

(b) 400−600 °C. Heating at 400−500 °C for 6 h (parts d and e of Figure 1) causes the full destruction of the layer structure of the original LDH and the formation of additional crystalline LiCl. The broad band from 20° to 50° 2θ decreases in intensity with increasing temperature, and peaks near 38°, 46°, 62°, and 67° 2θ become more pronounced and sharper. It is difficult, however, to unambiguously identify the ill-crystallized phases giving rise to these reflections because the peaks are broad and several potential Li-alumnate phases have similar *d* spacings. Both $LiAl_5O_8$ and α-$LiAlO_2$ have peaks near 38°, 46° (45.4° 2θ for α-$LiAlO_2$ and 45.9° 2θ for $LiAl_5O_8$, as shown in parts g−i of Figure 1), and 67° 2θ. The peak near 61° appears to be characteristic of $LiAl_5O_8$ (511),[20] and volumes with a structure similar to it first come into existence at least by 500 °C. At 600 °C (Figure 1f), a broad peak at 19° unambiguously representing α-$LiAlO_2$ (JCPCD 19-713) first becomes well resolved. The observed DSC endotherm at 540 °C (Figure 2a−c) may be related to the formation of the α-$LiAlO_2$ and $LiAl_5O_8$ phases, which could occur at lower temperatures during static heating for 6 h.

(c) 720−1100 °C. All of the observed Bragg peaks in this temperature range can be assigned unambiguously, although there is still some broad intensity from 20° to 50° 2θ at 720 and 850 °C. The reflections at 19° 2θ representing α-$LiAlO_2$ are well-defined, reach their maximum relative intensity at 720 °C (Figure 1g), decrease at higher temperatures, and are not present at 1100 °C. Well-resolved reflections for $LiAl_5O_8$ at 39.5° (222) and 45.9° (400) 2θ (JCPCD 38-1425) first appear at 720 °C (Figure 1g). The relative intensities of these reflections increase with increasing temperature, and at 1100 °C, $LiAl_5O_8$ is the dominant phase (Figure 1j). Its (110) and (210) peaks near 16° and 26° 2θ are superlattice reflections and signify an ordered distribution of 1Li and 3Al over the octahedral sites of this inverse-spinel structure.[6,21] They appear here only for the samples heated at 970 °C and above. At 1100 °C, a minor new phase, γ-$LiAlO_2$, with characteristic reflections at 22.3°, 33.4°, and 34.7° 2θ appears (JCPCD 38-1464).

NMR Spectra. (a) ^{27}Al MAS NMR Spectra. The ^{27}Al MAS NMR spectra of the samples are in good agreement with the TG/DSC and XRD data. The spectrum of a room-humidity sample of $LiAl_2(OH)_6Cl{\cdot}nH_2O$ shows a narrow symmetric peak at both high field ($H_0 = 17.6$ T) and lower field ($H_0 = 11.74$ T, data not shown), with a maximum at 8.6 ppm at $H_0 = 17.6$ T (Figure 3a). There are no singularities that would allow for the determination of the quadrupolar coupling parameters. This chemical shift is typical of six-coordinated Al (Al[6]),[22] in

(20) Famery, R.; Queyeoux, F.; Gilles, E. J.-C.; Herpin, E. P. *J. Solid State Chem.* **1979**, *30*, 257−263.
(21) Nageswara Rao, E.; Ghose, J. *Mater. Res. Bull.* **1986**, *21*, 55−60.
(22) Kirkpatrick, R. J. In *Spectroscopy Methods in Mineralogy and Geology*; Hawthorne, F. C., Ed.; Mineralogical Society of America: Washington, DC, 1988; Vol. 18, pp 341−403.

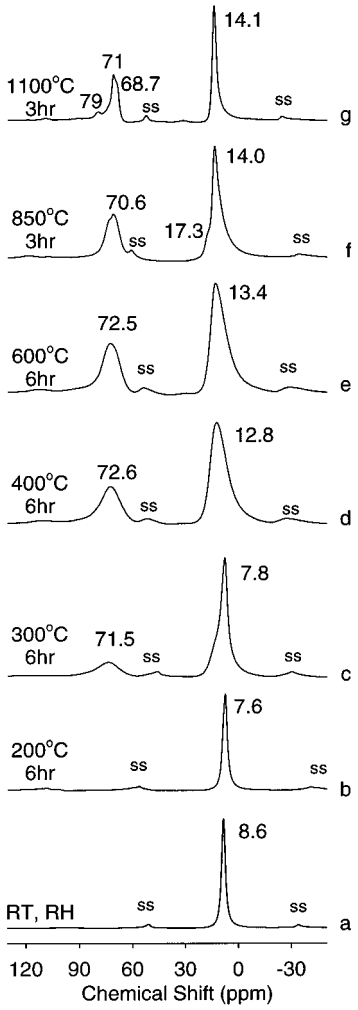

Figure 3. ^{27}Al MAS NMR spectra (H_0 = 17.6 T) of $LiAl_2(OH)_6Cl\cdot nH_2O$ (LiAlCl8) and its products calcinated under the conditions indicated (ss, spin sidebands).

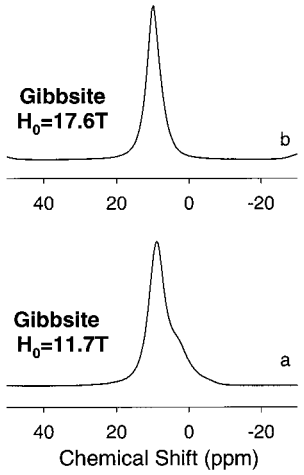

Figure 4. ^{27}Al MAS NMR spectra of starting gibbsite collected at (a) H_0 = 11.7 T and (b) H_0 = 17.6 T.

agreement with the known structure of this phase.[11,12] The narrow, symmetric peak indicates that Al occupies highly ordered and symmetric octahedral positions. In contrast, the ^{27}Al spectra of the gibbsite used to synthesize the LDH are broader (Figure 4), and previous two-dimensional multiple-quantum ^{27}Al experiments show that gibbsite yields two resonances with similar isotropic chemical shifts (ICSs) of 11 and 12 ppm but

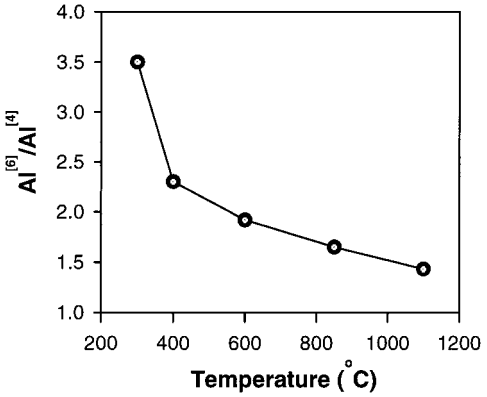

Figure 5. Molar ratios of Al[6]/Al[4] as a function of the heating temperature as determined by the curve fitting of the 17.6 T MAS NMR spectra.

different quadrupolar products (P_Q) of 2.2 and 4.7 MHz.[23] These arise from the two crystallograpically distinct Al sites in gibbsite.[24] These observations indicate that Li^+ for vacancy substitution leads to a more uniform distribution of a positive charge within the octahedral sheet, thereby reducing the differences among individual Al−O bond lengths and O−Al−O bond angles. In the Reitveld refinements of powder XRD data,[12] the Al−O bond lengths in the hydrated $LiAl_2(OH)_6Cl\cdot nH_2O$ phase range only from 1.898 to 1.911 Å, and those in the dehydrated $LiAl_2(OH)_6Cl$ phase are all 1.888 Å.[12] In contrast, in gibbsite, they range from 1.862 to 1.947 Å.[24] The ^{27}Al MAS NMR spectra of samples heated at 200 °C and below, corresponding to the fully dehydrated form, are similar to those of ambient samples (Figure 3b, only 200 °C spectrum shown), indicating that the hydroxide-layer structure remains unchanged in this temperature range, consistent with the XRD and TA data discussed previously. The peak maximum is displaced only about 1−7.6 ppm due to dehydration.

At 300 °C (Figure 3c), a low and broad resonance with a peak maximum at 71.5 ppm representing four-coordinated Al (Al[4])[22] appears, and an additional Al[6] resonance occurs as a shoulder at about 13 ppm to the left of the main peak at 7.8 ppm. These resonances are consistent with the XRD data, indicating the formation of an amorphous phase at this temperature along with the persistence of some $LiAl_2(OH)_6Cl$. As is often observed for amorphous hydrous aluminate materials,[25] this amorphous phase contains both Al[4] and Al[6]. No Al[5] is observed for any of our samples at any temperature. At 400 °C, only the broad 73 and 13 ppm peaks are present, and there is no signal for residual LDH, consistent with the XRD data. At 600 °C, the spectrum is essentially the same as that at 400 °C except that the apparent Al[6]/Al[4] ratio determined from peak areas in the 17.6 T MAS spectra decreases from 2.3 to 1.9 (Figure 5).

At 850 °C, the Al[6] and Al[4] resonances are narrower and better resolved. Al[6] resonances with peak maxima at 17.3 and 14 ppm can be distinguished, and there is a poorly resolved structure in the Al[4] peak. At 1100 °C, the peaks are even narrower, the resonance at 17 ppm is no longer present, and, additionally, there is a small peak at 79.3 ppm and a very small shoulder at 73 ppm. From 850 to 1100 °C, the overall Al[6]/

(23) Ashbrook, S. E.; McManus, J.; MacKenzie, K. J. D.; Wimperis, S. *J. Phys. Chem. B* **2000**, *104*, 6408−6416.
(24) Saalfeld, H.; Wedde, M. *Z. Kristallogr., Kristallgeom., Kristallphys., Kristallchem.* **1974**, *139*, 129−35.
(25) Yokoyama, T.; Nishui, K.; Torii, S.; Ikeda, Y.; Watanabe, T. *J. Mater. Res.* **1997**, *12*, 2111−2116.

Al[4] ratio decreases from 1.65 at 850 °C to 1.43 at 1100 °C (Figure 5), indicating that Al redistribution is still occurring in this temperature range.

The observed ^{27}Al MAS NMR behavior reflects the structural evolution of the phases present and is consistent with the XRD and TA data. Dehydroxylation begins near 300 °C, and after heating at this temperature for 6 h, a significant amount of the OH^- is lost and much of the LiCl is exsolved. Dehydroxylation results in the formation of both Al−O tetrahedra and octahedra but in contrast to the dehydration of aluminosilicate minerals such as kaolinite and pyrophyllite not Al[5].[26,27] At the intermediate stages, all of the Al-containing phases are amorphous or poorly crystalline and, thus, yield broader peaks than both the ambient LDH samples and the high-temperature phases.

At higher temperatures, the peak at 17 ppm at 850 °C (Figure 3f) is due to α-$LiAlO_2$, which has a distorted NaCl-like structure containing cross-linked sheets of alternating AlO_6 and LiO_6 octahedra,[3] in agreement with the single Al[6] peak for it. The other features are due to $LiAl_5O_8$ and have an Al[6]/Al[4] ratio of ∼1.5, consistent with its structure.[20,28] $LiAl_5O_8$ has an inverse-spinel structure, with 3Al and 1Li occupying the octahedral sites and the remaining 2Al occupying tetrahedral sites.[20] The signal in the 60−85 ppm range for the 1100 °C sample (Figure 3g) can be best simulated with two components with ICSs, quadrupole coupling constants (QCCs), and quadrupolar asymmetry parameters (η) of 82.5 ppm, 6.1 MHz, and 0.1 and of 72.6 ppm, 4.05 MHz, and 0.0, respectively. The first component is due to γ-$LiAlO_2$, which has a tetragonal structure containing Al[4] and Li[6].[1] The large QCC indicates that the Al tetrahedra are significantly distorted, consistent with XRD refinement data[29] and IR data.[5] The second component is due to Al[4] in $LiAl_5O_8$. The ICS and quadrupolar parameters for this phase found here are very similar to those of Stewart et al.[30] except that our ICS is 2 ppm more positive. Previously reported ^{27}Al MAS NMR spectra for γ-$LiAlO_2$[1,5] were interpreted to indicate the presence of two sites, but this interpretation is inconsistent with the XRD data that indicate a single Al site.[29] The previously reported spectra were taken at low field (7.05 T) and actually showed a well-defined second-order quadrupolar powder pattern.

(b) ^{6}Li and ^{7}Li MAS NMR. The ^{6}Li MAS NMR spectra of all of the samples have a very high resolution, and all of the observed spectral components are well simulated with symmetrical Lorenzian/Gausian peaks (Figure 6). The room-temperature samples and those heated at 200 °C and below have similar ^{6}Li spectra, with peak maxima between −0.04 and −0.06 ppm (parts a and c of Figure 6) and a full width at half-height (fwhh) of ∼90 Hz. For the ambient sample in paste form, the resonance (Figure 6b) remains at the same frequency but narrows to a fwhh of ∼53 Hz. These observations indicate that the local Li structural environments are not significantly affected by hydration state and temperature in this range, as is also observed for Al[6]. This chemical shift is in the range expected for Li[6],[14,15] consistent with the structure of $LiAl_2(OH)_6Cl\cdot nH_2O$.[10−12] The 300 °C sample (Figure 6d) yields this peak, a resolvable component at −0.40 ppm, and a narrow peak with a maximum at −1.10 ppm and a fwhh of 35 Hz. The latter is readily assigned to the crystalline LiCl observed in the XRD patterns (Figure 1) and is present at all of the temperatures up to 970 °C, where its relative intensity decreases significantly. The peak at −0.40 ppm must be due to Li in the amorphous Li-aluminate phase detected by XRD and ^{27}Al NMR. At 400 °C (Figure 6e), only a broad peak for the amorphous phase centered at 0 ppm and the LiCl peak at −1.1 ppm occurs.

From 500 to 970 °C, all of the spectra can be well simulated with two components with chemical shifts of 0.31 and −0.4 ppm, in addition to the peak for LiCl at −1.1 ppm. On the basis of their variation in relative intensity with calcination temperature and a comparison to the XRD data previously stated, the

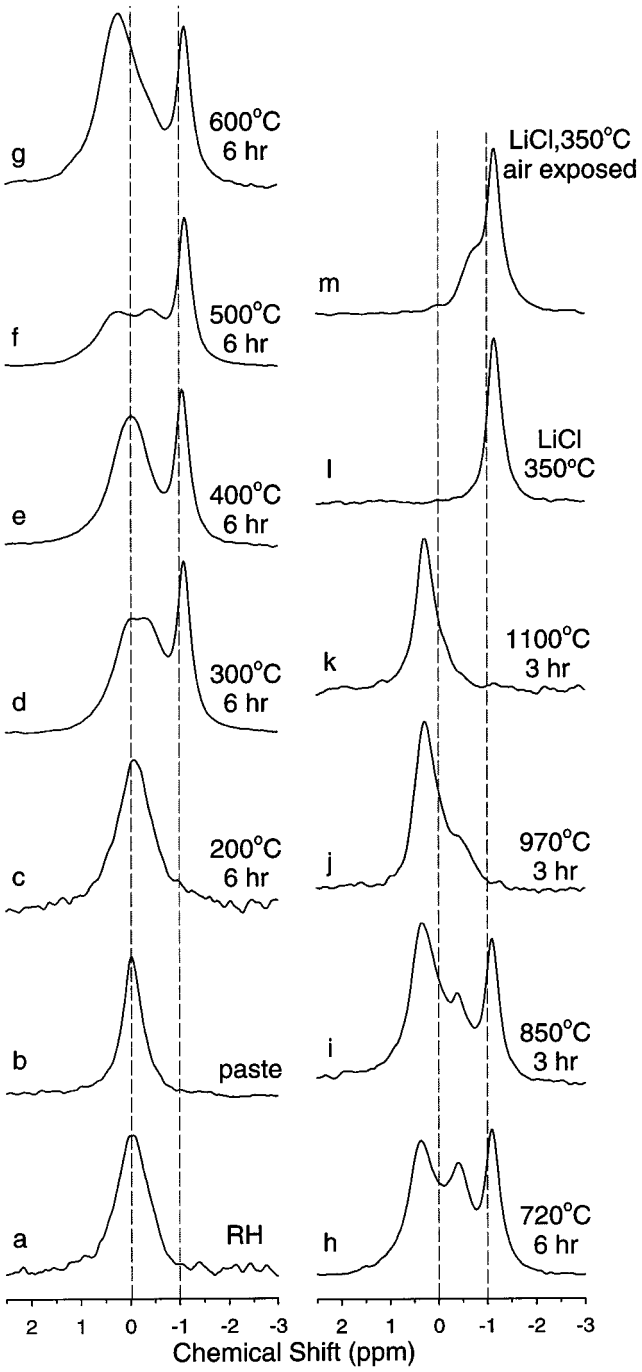

Figure 6. ^{6}Li MAS NMR spectra of $LiAl_2(OH)_6Cl\cdot nH_2O$ (LiAlCl8) and its products calcinated under the conditions indicated. Spectra l and m are for the LiCl salts. See the text for a detailed description.

(26) Lambert, J. F.; Millman, W. S.; Fripiat, J. J. *J. Am. Chem. Soc.* **1989**, *111*, 3517−3522.
(27) Fitzgerald, J. J.; Dec, S. F.; Hamza, A. I. *Am. Mineral.* **1989**, *74*, 1405−1408.
(28) Kriens, M.; Adiwidjaja, G.; Guse, W.; Klaska, K. H.; Lathe, C.; Saalfeld, H. *Neues Jahrb. Mineral., Monatsh.* **1996**, *8*, 344−350.
(29) Bertaut, F.; Delapalme, A.; Bassi, G.; Durif-Varambon, A.; Joubert, J. C. *Bull. Soc. Fr. Mineral. Cristallogr.* **1965**, *88* (1), 103−8.
(30) Stewart, F. F.; Stebbins, J. F.; Peterson, E. S.; Farnan, I.; Dunham, S. O.; Adams, E.; Jennings, P. W. *Chem. Mater.* **1995**, *7*, 363−367.

resonance at −0.4 ppm is readily assigned to α-$LiAlO_2$ and that at 0.31 ppm to $LiAl_5O_8$ (Table 1). Their fitted peak widths (fwhh) decease by about a factor of 2 with an increase in the heating temperature, paralleling their progressively improving crystallinity observed by XRD. The line fit of the 850 °C spectrum (Figure 6i) yields a molar ratio of $LiAl_5O_8$/α-LiAlO2/LiCl of 3.13/1/1.27, implying a molar Al/Li ratio of 3.08 if these are the only phases present and if they are stoichiometric. This value is close to that from the compositional analysis, 2.85. The 1100 °C spectrum (Figure 6k) can be fairly well simulated with two components, one at 0.31 ppm for $LiAl_5O_8$ and one at −0.06 ppm for γ-$LiAlO_2$ (Table 1), although there still might be a small amount of signal at −0.4 ppm from residual α-$LiAlO_2$. The molar ratio of $LiAl_5O_8$/γ-$LiAlO_2$ in the 1100 °C sample determined from the ^{6}Li peak areas is about 3.09, yielding a molar Al/Li ratio of 4.02 which is again in reasonably good agreement with the compositional analyses (molar Al/Li = 4.52). These values are also in agreement with the simulation of the ^{27}Al NMR spectrum of the two samples, although the precision of this simulation is probably poorer because of peak overlap and quadrupolar effects.

Hydrated lithium chloride, LiCl·H_2O, which was observed in the XRD patterns, resonates at −0.6 ppm (Figure 6m) but is not observed in the NMR samples because they were not significantly exposed to air. Figure 6m shows the ^{6}Li MAS NMR spectrum of heated LiCl salt (Figure 6l) exposed to air for ∼60 min. It contains three components representing solution-like LiCl at 0 ppm (trace), LiCl·H_2O at −0.6 ppm, and LiCl at 1.1 ppm.

The ^{6}Li chemical shifts indicate that essentially all of the Li in the calcined samples retain the sixfold coordination of the LDH. ^{6}Li has a very small quadruple moment; thus, the observed peak maxima are very close to the isotropic chemical shifts.[14,15] The correlation between coordination number (CN) and ^{6}Li chemical shifts has been established for Li-containing silicate/aluminosilicate[14] and lithium phosphate glasses[15] but may not fully apply to aluminate systems. On the basis of the known effects of Al, Si, and P on the chemical shifts of other cations to which they are connected through M−O−M bonds,[22] the ^{6}Li ICSs should be slightly more positive for aluminate systems than for aluminosilicate or phosphate systems. The isotropic chemical shifts of 0.31 ppm for $LiAl_5O_8$, −0.06 ppm for γ-$LiAlO_2$, and −0.4 ppm for α-$LiAlO_2$, all of which contain Li in only sixfold coordination,[3,20,28,30] are in the range or are deshielded relative to the −0.3 to −1.3 and −0.7 to −1.5 ppm chemical shift range of Li[6] in aluminosilicates[14] and phosphate glasses,[15] consistent with this idea. This result implies that Li in the amorphous phase present at 300 and 400 °C is also six-coordinated because its peak maxima are in the range −0.04 to −0.40 ppm.

The ^{7}Li MAS NMR spectra for samples heated at 400 °C and below are very similar to the ^{6}Li spectra except that the peaks are much broader (e.g., ∼900 Hz fwhh for the RH = 0% LDH sample, 568 Hz for the RH = 75% sample, and 446 Hz for LiCl formed from LDH (spectra not shown)). The chemical shifts (peak maxima) are almost identical to those of ^{6}Li (e.g., −1.06 ppm for ^{7}LiCl and −0.03 ppm for room humidity LDH). Thus, we do not discuss them in detail. Simulation of the ^{7}Li MAS NMR spectra of the 300 and 400 °C samples yields relative resonance intensities similar to those from ^{6}Li MAS NMR. Because the ^{7}Li spectra were obtained with a single scan, there was no spin saturation, and the similarity of the relative intensities provides confidence in the relative intensities from the ^{6}Li data, even though the T_1 values are long and unknown.

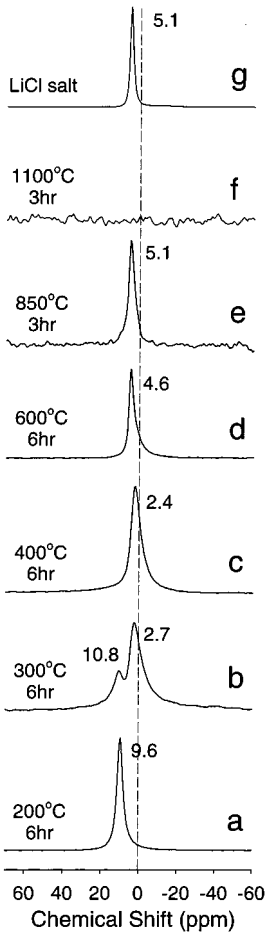

Figure 7. ^{35}Cl MAS NMR spectra of $LiAl_2(OH)_6Cl{\cdot}nH_2O$ (LIALC8) and its products calcinated under the conditions indicated. The spectrum g (top) is for the as-purchased LiCl salt.

(c) ^{35}Cl MAS NMR Data. The ^{35}Cl MAS NMR spectra (Figure 7) provide important information about the Cl^- sites present in the various samples. The spectrum of the dehydrated 200 °C sample (Figure 7a) contains a single, symmetrical, narrow peak with a maximum at 9.6 ppm, as expected for the well-ordered structure of this phase.[12] The 300 °C sample (Figure 7b) yields this peak (maximum at 10.8 ppm) and a broader peak with a maximum at 2.7 ppm. The latter peak is the only one for the 400 °C sample (Figure 7c). At 600 °C (Figure 7d), the peak is narrower, has a maximum at 4.6 ppm, and is slightly skewed to less positive values. At 850 °C (Figure 7e), the peak is narrow and symmetrical and has a maximum of 5.1 ppm, identical to that of crystalline LiCl (Figure 7g). The 1100 °C sample (Figure 7f) yields no ^{35}Cl signal, consistent with the absence of LiCl indicated by the ^{6}Li NMR data. By comparison with the XRD data, we interpret the peaks with maxima varying from 2.7 to 5.1 ppm to be due to Cl^- in LiCl crystallites. At the lower temperatures, the peak maximum is probably displaced to the right because of quadrupolar effects associated with disorder or small particle size.

Structural Transformations

Taken together, the compositional, XRD, TG/DSC, and NMR data indicate the following set of transformations for the $LiAl_2(OH)_6Cl{\cdot}nH_2O$ LDH phase.

(1) Dehydration (loss of surface and interlayer water molecules) via the reaction $LiAl_2(OH)_6Cl{\cdot}nH_2O \rightarrow LiAl_2(OH)_6Cl$

+ nH_2O begins near room temperature, depending on RH, and culminates near 125 °C in our DSC/TG scans.

(2) Decomposition of the dehydrated LDH occurs via the reaction $LiAl_2(OH)_6Cl \rightarrow$ amorphous $Li_{1-x}Al_2O_{6-y}H_{6-2y-z} + xLiCl_s + yH_2O_g + zHCl_g$ beginning at temperatures of less than 300 °C. At 400 °C, most of the water and HCl loss is complete. The XRD and NMR data indicate that the Li/Al phase is quite amorphous at this temperature. Our DSC/TG unit is not equipped with a mass spectrometer; thus, the volatile HCl was not positively identified. However, without the occurrence of redox reactions for which there is no evidence, there is no other way to fully remove the Cl without also removing all of the Li as LiCl. The Li/Cl ratio of the starting LDH is 1/1, and because Li is present in the high-temperature oxides, some of the Cl must be lost as HCl.

(3) Formation of domains with the α-$LiAlO_2$ and $LiAl_5O_8$ structures begins by at least 500 °C in the samples heated for 6 h and probably gives rise to the 540 °C peak in the DSC data. This transformation is best seen in the ^{6}Li NMR spectra. These domains are probably initially small and highly disordered.

(4) There is a progressive ordering and recrystallization of the α-$LiAlO_2$ and $LiAl_5O_8$ phases with increasing temperature. These processes are clearly seen in the progressive narrowing of the XRD peak widths, in the resolution of the Bragg peaks for both of the phases at 720 °C, and in the decreased peak widths and increased resolution in the ^{6}Li and ^{27}Al NMR spectra. The better resolution of the XRD pattern for α-$LiAlO_2$ compared to $LiAl_5O_8$ at 720 °C suggests that α-$LiAlO_2$ becomes better ordered at a lower temperature. TG data indicate a progressive weight loss to temperatures of above 600 °C associated with this reorganization. This weight loss is probably due to the loss of OH groups or water molecules. The appearance of the (110) peak for $LiAl_5O_8$ at 970 °C is the result of the ordering of Li and Al on the octahedral sites.

(5) Volatilization of LiCl begins at about 850 °C and culminates between 1000 and 1048 °C at the 10 °C min^{-1} heating rate of our DSC/TG scan. Because of this delithiation, the final products of the breakdown of the $LiAl_2(OH)_6Cl{\cdot}nH_2O$ LDH phase studied here are dominated by $LiAl_5O_8$. This contrasts with previous studies of the breakdown of $LiAl_2$ LDHs intercalated with OH^-,[1,7] NO_3^-,[7] and CO_3^{2-} [8] for which delithiation does not occur because the volatile products are only H_2O, NO_x, and CO_2. For these phases, the calcination products are dominated by $LiAlO_2$ and have a $LiAlO_2/LiAl_5O_8$ molar ratio of 3/1.[1,7,8]

(6) There is a transformation of α-$LiAlO_2$ to γ- $LiAlO_2$ between 970 and 1100 °C. This transition is well resolved in the XRD and NMR data and may contribute to the DSC signal near 1000 °C.

Acknowledgment. This research is supported by DOE Grant DEFG02-00ER15028 (R.J.K., Principal Investigator). Reviews by two anonymous reviewers substantially improved the manuscript.

IC010671D